THE JOURNAL OF BIOLOGICAL CHEMISTRY VOL. 284, NO. 6, pp. 3966–3975, February 6, 2009

Retinoschisin, a New Binding Partner for L-type Voltage-gated Calcium Channels in the Retina*

Received for publication, August 15, 2008, and in revised form, December 10, 2008 Published, JBC Papers in Press, December 11, 2008, DOI 10.1074/jbc.M806333200

Liheng Shi[‡1], **Kuihuan Jian**[‡1], **Michael L. Ko**[‡], **Dorothy Trump**[§], **and Gladys Y.-P. Ko**[‡2]

From the [‡]*Department of Veterinary Integrative Biosciences, College of Veterinary Medicine and Biomedical Sciences, Texas A&M University, College Station, Texas 77843-4458 and the* [§]*Medical Genetics Research Group and Centre for Molecular Medicine, Faculty of Medical and Health Sciences, University of Manchester, Manchester M13 9PT, United Kingdom*

The L-type voltage-gated calcium channels (L-VGCCs) are activated under high depolarization voltages. They are vital for diverse biological events, including cell excitability, differentiation, and synaptic transmission. In retinal photoreceptors, L-VGCCs are responsible for neurotransmitter release and are under circadian influences. However, the mechanism of L-VGCC regulation in photoreceptors is not fully understood. Here, we show that retinoschisin, a highly conserved extracellular protein, interacts with the L-VGCCα1D subunit and regulates its activities in a circadian manner. Mutations in the gene encoding retinoschisin (*RS1*) cause retinal disorganization that leads to early onset of macular degeneration. Since ion channel activities can be modulated through interactions with extracellular proteins, disruption of these interactions can alter physiology and be the root cause of disease states. Co-immunoprecipitation and mammalian two-hybrid assays showed that retinoschisin and the N-terminal fragment of the L-VGCCα1 subunit physically interacted with one another. The expression and secretion of retinoschisin are under circadian regulation with a peak at night and nadir during the day. Inhibition of L-type VGCCs decreased membrane-bound retinoschisin at night. Overexpression of a missense *RS1* mutant gene, R141G, into chicken cone photoreceptors caused a decrease of L-type VGCC currents at night. Our findings demonstrate a novel bidirectional relationship between an ion channel and an extracellular protein; L-type VGCCs regulate the circadian rhythm of retinoschisin secretion, whereas secreted retinoschisin feeds back to regulate L-type VGCCs. Therefore, physical interactions between L-VGCCα1 subunits and retinoschisin play an important role in the membrane retention of L-VGCCα1 subunits and photoreceptor-bipolar synaptic transmission.

Interactions between ion channels and extracellular proteins play important roles in the modulation of ion channel gating and synaptic plasticity. For example, extracellular matrix and cell adhesion proteins, such as integrin, regulate L-type voltage-gated calcium channel (VGCC)[3] functions in vascular smooth muscles (1–3). Likewise, in mice deficient for the extracellular matrix glycoprotein tenascin-C, the L-type VGCC-dependent form of synaptic plasticity in the hippocampus is impaired (4). In vertebrate retinas, retinoschisin is an extracellular adhesion protein secreted primarily from photoreceptors and bipolar cells and is distributed throughout the retina (5–8). After secretion, retinoschisin localizes mainly to the surface of photoreceptors and bipolar cells in adults (9). Mutations in retinoschisin (*RS1*) cause X-linked retinoschisis (XLRS), a retinal dystrophy that features disorganization of retinal cell layers, disruption of the synaptic structures and neurotransmission between photoreceptors and bipolar cells, and progressive degeneration of rod and cone photoreceptor cells (7, 10–14). Hence, retinoschisin is believed to play an important role in the development and maintenance of retinal cytoarchitecture (7, 8, 15). An interesting clinical aspect of XLRS is that it shares several quantifiable features with X-linked incomplete congenital stationary night blindness (XLCSNB), which is an inherited retinal dystrophy with a mutation in the L-type VGCCα1 subunit gene (16, 17). The electroretinogram (ERG) recordings from XLRS and XLCSNB patients are comparable, and in both cases, the cone photoreceptor responses are more severely affected than the rod responses, and synaptic transmission between photoreceptors and bipolar cells is severely damaged (18). Therefore, we postulated that molecular interactions between L-type VGCCs and retinoschisin may have an important impact in the synaptic transmission between photoreceptors and bipolar cells.

Visual systems must be able to detect images despite large daily changes in ambient illumination between day and night. Biological clocks (circadian oscillators) in the retina provide a mechanism that allows the visual system to anticipate these daily changes in photon flux by modulating retinal structure

* This work was supported, in whole or in part, by National Institutes of Health, NEI Grant NIHRO1EY017452 (to G. Y.-P. K.). This work was also supported by a Department of Veterinary Integrative Bioscience Programmatic Development Minigrant (to G. Y.-P. K.) and the start-up fund from Texas A&M University (to G. Y.-P. K.). The Image Analysis Laboratory has been supported in part by National Institutes of Health Grants S10RR022532, P42ES004917, and P30ES009106. The costs of publication of this article were defrayed in part by the payment of page charges. This article must therefore be hereby marked "*advertisement*" in accordance with 18 U.S.C. Section 1734 solely to indicate this fact.

The nucleotide sequence(s) reported in this paper has been submitted to the GenBank™/EBI Data Bank with accession number(s) EU924185.

[1] Both of these authors contributed equally to this work.

[2] To whom correspondence should be addressed: Dept. of Veterinary Integrative Biosciences, College of Veterinary Medicine and Biomedical Sciences, Texas A&M University, Mail Stop 4458, College Station, TX 77843-4458. Tel.: 979-845-2828; Fax: 979-847-8981; E-mail: gko@cvm.tamu.edu.

[3] The abbreviations used are: VGCC, voltage-gated calcium channel; L-VGCC, L-type VGCC; VGCCα1D, L-type voltage-gated calcium channel α1D subunit; XLRS, X-linked retinoschisis; XLCSNB, X-linked incomplete congenital stationary night blindness; IP, immunoprecipitation; ERG, electroretinogram; aa, amino acid(s); GFP, green fluorescent protein; EST, expressed sequence tag; RACE, rapid amplification of cDNA ends; PBS, phosphate-buffered saline; LD, light/dark; DD, constant darkness; CT, circadian time(s); E*n*, embryonic day *n*.

and physiology (19, 20). Retina photoreceptors are nonspiking neurons, and the continuous release of glutamate in the dark is a result of depolarization-evoked activation of L-type VGCCs (21). In avian retina photoreceptors, the circadian rhythms in the synthesis and release of melatonin are also L-type VGCC-dependent (22, 23). There is a diurnal rhythm of L-type VGCC currents in the goldfish retina with average peak amplitudes significantly larger at midnight than at midday (24). In chick retinas, expression of L-type VGCCα1 subunit transcripts and proteins is under circadian control, and the current amplitudes and the VGCCα1 subunit expression in cone photoreceptors are higher during the subjective night than during the subjective day (25). Previously, we showed that retinoschisin mRNA and protein expression and secretion are also under circadian control (26). Intriguingly, the rhythmic expression and secretion of retinoschisin is coincident with the circadian regulation of L-VGCCs in chick photoreceptors (25, 26), and the circadian-regulated secretion of retinoschisin is an L-type VGCC-dependent process; inhibition of L-type VGCCs dampens the circadian rhythm of retinoschisin secretion, where only night time secretion is affected (26). These observations led us to investigate the molecular and functional interactions between L-VGCCα1 subunits and retinoschisin and their functional aspects.

In this study, we present the first reported evidence for a novel reciprocal relationship between an ion channel and an extracellular protein; L-type VGCCs govern the circadian rhythm of retinoschisin secretion, whereas secreted retinoschisin ensures the circadian regulation of L-type VGCCs in the retina photoreceptors. The physical interactions between VGCCα1D N-terminal fragment and retinoschisin underlie a positive feedback regulation on each other. Since the N-terminal fragments among L-type VGCCα1C, -1D, and -1F are highly conserved, retinoschisin may very well interact with all three VGCCα1 subunits. Hence, physical interactions between L-VGCCα1 subunits and retinoschisin may play an important role in the membrane retention of VGCCα1 subunits and photoreceptor-bipolar synaptic transmission. Interactions between ion channels and extracellular proteins not only modulate ion channel activities, they may also dictate the physiology and function of cells, and the loss of such interactions may contribute to the cause of a disease state. We also cloned the full-length retinoschisin gene *rs1* from chickens (*Gallus gallus*) and found that retinoschisin is highly conserved among chickens, mice, and humans, and therefore, retinoschisin may be very important in retina function and physiology across species.

EXPERIMENTAL PROCEDURES

Cloning of Full-length Chicken rs1 Gene—Genomic comparisons between human, mouse, and chicken retinoschisin (*rs1*) gene loci were made through the University of California Santa Cruz genomic research program (available at the University of California Santa Cruz web site). A commercially available kit (Qiagen, Valencia, CA) was used to isolate total RNA from chicken retina (E18), 1 μg of which was used for reverse transcription (Superscript II; Invitrogen). Highly conserved regions among the different species and a partial high homolog cDNA fragment from chicken eye expressed sequence tag (EST; NCBI entry AI438129) were used to design the RT-PCR primers for amplification of chicken *rs1* (forward, 5′-AGGATGAGAGACTGGAGCTGTGGCAC-3′; reverse, 5′-CTCGTCGGGGTTGGAGCAGCTGATC-3′). 5′- and 3′-rapid amplification of cDNA ends (RACE) systems (Invitrogen) were used for tracing the 5′- and 3′-ends of the gene (5′-RACE, forward (5′-GGCCACGCGTCGACTAGTACGGGIIGGGIIGGGIIG) and reverse (5′-CTGCTCGGGGTTGGAGCAGCTGATC-3′); 3′-RACE, forward (5′-AGGATGAGAGACTGGAGCTGTGGCAC-3′) and reverse (5′-GGCCACGCGTCGACTAGTACTTTTTTTTTTTTTTTT-3′)). Amplification of gene products was achieved through 35 cycles of PCR. The PCR products were purified by the Qiaquick gel extraction kit (Qiagen) and cloned into pGEM-T easy vector (Promega, Madison, WI) for DNA sequencing (Gene Technologies Laboratory, Institute of Development and Molecular Biology, Texas A&M University, College Station, TX).

Immunohistochemistry—Chick E18 eyes were enucleated and fixed with Zamboni's fixative (Newcomer Supply, Middleton, WI) overnight at 4 °C followed by submerging with 10, 20, and 30% sucrose-PBS (0.1 M phosphate-buffered saline, pH 7.4) for cryoprotection. Whole eye sections (10 μm) were incubated with a primary antibody against retinoschisin (retinoschisin H-65 antibody; Santa Cruz Biotechnology, Inc., Santa Cruz, CA) at a dilution of 1:250 in 1% normal goat serum at 4 °C overnight. The tissue sections were washed in PBS several times and incubated with fluorescent conjugated secondary antibody (Alexa 488 nm goat anti-rabbit, 1:1500 dilution; Molecular Probes) for 2 h in the dark. After several washes, coverslips were mounted and stored at 4 °C for later observation on a Zeiss microscope with epifluorescence to determine the distribution of retinoschisin.

Circadian Entrainment and Cell Culture—Fertilized eggs (*G. gallus*) were obtained from the Poultry Science Department (Texas A&M University, College Station, TX). Chick embryos from embryonic day 11 (E11) were entrained to 12 h/12 h light/dark (LD) cycles at 39 °C *in ovo*. Zeitgeber time 0 was designated as the time when the lights came on, and Zeitgeber time 12 was the time when the lights went off. After *in ovo* LD entrainment for 6 days, eggs were kept in constant darkness (DD) for another day. On the second day of DD, retinas were dissected out for biochemistry or molecular biology analysis at various circadian times (CT) of the day. In some experiments, on the last day of LD entrainment, retinal cells were dissociated, cultured in DD (39 °C, 5% CO_2) as described previously (27, 28), and used for biochemistry assays on the second day of DD.

Cell Surface Biotinylation Assay and Western Blot Analysis—A commercially available cell surface biotinylation assay kit (Pierce) was used, and the manufacturer's instructions were followed to determine the relative amount of retinoschisin bound to the cell membrane as a function of circadian time. By only labeling cell surface proteins, this assay allows for independent analysis of cell surface and cytosolic fractions of proteins (29). For this study, we also assessed retinoschisin of the whole lysate (membrane plus cytosolic fractions). Nitrendipine (Sigma) is a VGCC inhibitor and was used to partially gauge any interaction between retinoschisin and VGCCs. This drug (or control vehicle) was added to retina cultures at CT 3 and 15. After 2 h, cultured cells were washed with ice-cold PBS (pH 8.0)

and exposed to sulfosuccinimidyl-6-(biotinamido) hexanoate (2 mM) for 60 min on an ice bath inside a 4 °C refrigerator to label all cell surface proteins, followed by termination of biotinylation with 100 mM glycine-PBS for 10 min. After lysis, most of the lysate was used to determine the relative amount of plasma membrane-bound retinoschisin by incubating it with streptavidin-linked agarose beads. As a control, the agarose beads were incubated with lysates where cells were not exposed to the biotin. The beads were collected, and the amount of retinoschisin was determined by Western immunoblotting. A small portion of the whole cell lysate was used to measure retinoschisin and total Erk. The Western blotting process has been described previously (25–28, 30). Briefly, samples were separated on 10% SDS-polyacrylamide gels and transferred to nitrocellulose membranes. The primary antibodies used for this part of the present study were anti-retinoschisin (generated in the Trump laboratory) (5) and a polyclonal antibody insensitive to the phosphorylation state of Erk (total Erk, used for loading control; Santa Cruz Biotechnology). Blots were visualized with an anti-rabbit secondary antibody conjugated to horseradish peroxidase (Cell Signaling, Danvers, MA) and an ECL detection system (Pierce). The ratio of retinoschisin to total Erk in each sample was determined by densitometry with Scion Image software (National Institutes of Health, Bethesda, MD). All measurements were repeated 5–6 times.

Co-immunoprecipitation and Mammalian Two-hybrid Assays—To determine whether retinoschisin physically interacted with VGCCs, co-immunoprecipitation (co-IP) and mammalian two-hybrid assays were performed. For co-IPs, eight retinas (from either CT 5 or CT 17) were collected and homogenized in 1 ml of lysis buffer (1% Nonidet P-40). Samples were rotated at 4 °C for 3 h to solubilize membrane proteins. Samples were then centrifuged to remove cell debris, and a small portion of the supernatant was taken for protein assay analysis and for use in a Coomassie-stained gel. The rest of the supernatant was precleared with Protein A-agarose (GBiosciences, Maryland Heights, MO). The beads were removed, and 5 μl of antibody (anti-retinoschisin or anti-VGCCα1D) were added and incubated for 3 h. No antibody was added to the control groups. After antibody incubation, 20 μl of Protein A-agarose were added to each tube and incubated for another 1.5 h. The beads were collected and processed for Western blot analysis of retinoschisin and VGCCα1D. The supernatant was also saved and processed for Western blot analysis of total Erk. In addition to retinoschisin and total Erk antibodies, anti-VGCCα1D and anti-VGCCpanα1 (Alomone, Jerusalem, Israel) were used for these experiments. The epitope of the anti-VGCCα1D antibody contains 17 amino acids (aa), with 12 residues homologous to the chicken VGCCα1D subunit. The anti-panα1 antibody recognizes all VGCCα1 subtypes and contains 19 amino acids with 100% homology to the chicken VGCCα1C and -α1D subunits. The anti-retinoschisin antibody used in the co-IPs was generated in the Trump laboratory (5). Western blots were visualized as above. For some IPs, antibody preparatory and immunoprecipitation kits (Pierce) were used to remove heavy and light chain interference so that larger blot images could be shown. A commercially available kit (Bio-Rad) following the Bradford method was used to determine total protein content of the samples. All co-IPs were repeated three times.

For the mammalian two-hybrid assay, N (bp 1–1481 from ATG) and C termini (bp 5100–6573 ending in TAG) of VGCCα1D (Gene ID 395895) were amplified by reverse transcription-PCR from 2 μg of chicken heart total RNA. The primers for the N terminus were 5′-CGGGGATCCTGCAGCACCACCAGCAGCAGCAG-3′ (forward) and 5′-GTTTCTAGACTCGGTTTCGCTGGTGGGCATGC-3′ (reverse). The primers for the C terminus were 5′-AAAGGATCCCAGACGAGGAGGAGGAAGTTTA-3′ (forward) and 5′-GCTGGATCCTATAAGCTTGTAATGCATATCAT-3′ (reverse). The PCR products were purified (Qiaquick, Qiagen) and subcloned into pGEM-T-easy vectors (Promega) to confirm the sequence. The RS1 and VGCCα1D N or C termini were inserted into mammalian expression vectors pBind and pACT, respectively (Promega). The transfection reporter assay was carried out by a luciferase assay system (Promega). Briefly, three constructs, pBind or pBind-RS1, pACT or pACT-VGCCα1D, and pG5Luc (100 ng each) were cotransfected into Cos1 cells (TransIT®-COS transfection kit; Mirus, Madison, WI). After cells were harvested, 10 μl of the supernatant was mixed with luciferase substrate, and the relative luciferase activity was determined by luminosity (PerkinElmer Life Sciences). All luciferase assays were repeated seven times.

Biolistic Transfection and Electrophysiology—Chick retinas from E12 were dissociated, cultured, and entrained under LD cycles for 5 days and then kept in DD in the presence of 40 ng/ml ciliary neurotrophic factor (R&D Systems, Minneapolis, MN) and 15% heat-inactivated horse serum (25, 27, 28, 30). On the first day of DD, cells were transfected using a biolistic particle delivery system (Helium Gene Gun; Bio-Rad). Plasmids were precipitated onto 1.0-μm gold microcarriers according to the manufacturer's protocol. The particle delivery system generated a helium shock wave with a pressure gradient of 150 p.s.i. to accelerate the coated microcarriers onto cultured cells. After transfection, cells remained in culture under DD for another day before electrophysiological recordings were performed at CT 4–7 or 16–19 on the second day of DD. The plasmid encoding enhanced green fluorescent protein (GFP) is commercially available (Vitality® hrGFP II-1 Mammalian Expression Vector, catalog number 240143; Stratagene, La Jolla, CA). In these experiments, single missense mutants of human *RS1* genes, R141G and W92C (pCDNA3.1), were co-transfected with phrGFPII plasmid. All of these constructs use cytomegalovirus promoters. R141G and W92C were prepared in the Trump laboratory (13, 31).

For electrophysiological recordings, whole-cell patch clamp configuration of L-type VGCCs was carried out in an external solution containing the following: 110 mM NaCl, 10 mM $BaCl_2$, 0.4 mM $MgCl_2$, 5.3 mM KCl, 20 mM tetraethylammonium chloride, 10 mM HEPES, and 5.6 mM glucose, pH 7.4, with NaOH. The pipette solution was 135 mM cesium acetate, 10 mM CsCl, 2 mM $MgCl_2$, 0.1 mM $CaCl_2$, 1.1 mM EGTA, and 10 mM HEPES, pH 7.4, adjusted with CsOH (32). Recordings were made from cone photoreceptors characterized morphologically as cells with elongated cell bodies with one or more prominent oil droplets. Currents were recorded at room temperature using an Axopatch 200B amplifier (Axon Instruments/Molecular

Devices, Union City, CA). Signals were low pass-filtered at 2 kHz and digitized at 5 kHz with Digidata 1440A interface and pCLAMP 10.0 software (Axon Instruments). Currents were leak-subtracted. After gigaohm seals formed, the electrode capacitance was compensated. Current-voltage (*I*-V) relations were elicited from a holding potential of −65 mV in 200-ms steps (5 s between steps) to test potentials over a range of −80 to +60 mV in 10-mV increments. The membrane capacitance, series resistance, and input resistance of the recorded photoreceptors were measured by applying a 5-mV (100-ms) depolarizing voltage step from a holding potential of −65 mV. Cells with an input resistance <1 gigaohm were discarded. The membrane capacitance reading was used as the value for whole cell capacitance. The current densities of I_{Ba}^{2+} ($I_{density}$) were obtained by dividing the membrane capacitances from current amplitudes. Each group contained 9–18 cells.

TABLE 1

Full-length chicken, *G. gallus rs1* cDNA sequence

The complete chicken (*G. gallus*) retinoschisin (*rs1*) sequence contains 856 base pairs that encode 225 amino acids. The starting codon ATG is in blue underlined, and the stop codon TGA is in red underlined. The encoded amino acids are in boldface type.

```
gaattcgattggcccgcgtcgactagtacgggggggggggggggggggATTCCTGAAAG
GGGAAGGAAAAGATGCGGTTCAAGATGGGGAGAGTCCTGCTGTCTCTTCTTTTCTGGTAC
            M  R  F  K  M  G  R  V  L  L  S  L  L  F  W  Y
AAAGCTGTTCTGGCCCTGTCCCCTGGTGAGGATGAGAGACTGGAGCTGTGGCACAGCAAA
 K  A  V  L  A  L  S  P  G  E  D  E  R  L  E  L  W  H  S  K
GCTTGCAAATGCAATTGTCAGGGAGGTCCTAATTCAGTGTGGTCCAGCGGAACTAACAGC
 A  C  K  C  N  C  Q  G  G  P  N  S  V  W  S  S  G  T  N  S
TTGGAGTGCATGCCAGAGTGCCCCTACCACAAGCCCCTCGGCTTTGAGTCTGGCGCTGTC
 L  E  C  M  P  E  C  P  Y  H  K  P  L  G  F  E  S  G  A  V
ACCCCTGACCAGATCAGCTGCTCCAACCCCGAGCAGTACACAGGCTGGTACTCCTCATGG
 T  P  D  Q  I  S  C  S  N  P  E  Q  Y  T  G  W  Y  S  S  W
ACAGCCAATAAGGCCCGCCTCAACGGCCAAGGCTTTGGGTGCGCCCTGGCTCTCTCCAAG
 T  A  N  K  A  R  L  N  G  Q  G  F  G  C  A  L  A  L  S  K
TACCAGGACAACGGGCAGTGGCTGCAGATCGACCTGAAGGAGGTGAAGGTGATCTCAGGG
 Y  Q  D  N  G  Q  W  L  Q  I  D  L  K  E  V  K  V  I  S  G
ATCCTCACACAAGGGCGCTGTGATGCTGATGAGTGGATGACCAAATACAGCGTGCAGTAC
 I  L  T  Q  G  R  C  D  A  D  E  W  M  T  K  Y  S  V  Q  Y
CGCACAGATGAGAACCTCAACTGGGTTTACTACAAGGATCAGACCGGGAACAACCGGGTT
 R  T  D  E  N  L  N  W  V  Y  Y  K  D  Q  T  G  N  N  R  V
TTCTATGGCAACTCGGACCGGTCATCCTCAGTGCAGAACCTGCTGCGGCCGCCCATTGTG
 F  Y  G  N  S  D  R  S  S  S  V  Q  N  L  L  R  P  P  I  V
GCCCGCTACATCCGCCTCATCCCGCTGGGCTGGCACGTGCGCATTGCCATCCGCATGGAG
 A  R  Y  I  R  L  I  P  L  G  W  H  V  R  I  A  I  R  M  E
CTCCTCGAGTGCCTGGGCAAATGTGGCTGAGTGCCCCACTGGGTAGAGATGTGCAGGTGT
 L  L  E  C  L  G  K  C  G  *
GTGCCTGTATGGCCGTCCCATCTCACTGCTGATGCGTGCTGCGGCCACGATCCTGCCGAC
CCTACAAACAGAAGGGCTTTCTTGAATAAAACACTGCTTTACATGAAAAAAAAAAAAAAA
TAAAAgtactagtcgacgcgtggcc
```

Statistical Analysis—All of the data are presented as mean ± S.E. Student's *t* test or one-way analysis of variance followed by Tukey's *post hoc* test for unbalanced *n* was used for statistical analysis. Throughout, $p < 0.05$ (asterisk) was regarded as significant.

RESULTS

Retinoschisin Is Highly Conserved from Chickens to Humans—Human *RS1* and mouse *rs1* cDNAs are both composed of six exons occupying 32 kb. They share 90% homology in both nucleotide and amino acid sequences (GeneID: 6247 and 20147). We chose to use chicken retinas as our model in this study because chicken retinas are cone-dominant, and the cone pathways in the ERGs from XLRS and XLCSNB patients are more severely affected than the rod responses (18). Since the full-length chicken (*G. gallus*) *rs1* sequence was not available, we first used human *RS1* cDNA as a reference to search for high homology expressed mRNA fragments in chicken expressed sequence tags for cloning chicken *rs1*. One candidate cDNA fragment (AI438129) was the result from an NCBI cross-species megaBlast search. This fragment contains two exons, which can be traced to chicken chromosome 1 nucleotides 123,954,233–123,954,340 and 123,957,154–123,957,236, respectively. Using wide genomic sequence comparisons among different species, we were able to align highly conserved regions in humans, mice, and chickens (University of California Santa Cruz). Based on the genomic comparisons, we first designed a pair of primers to verify the *rs1* fragment (AI438129) from a chicken eye cDNA library. To clone full-length chicken *rs1* cDNA, we utilized 5′- and 3′-RACE assays to amplify the upstream and downstream sequences from this chicken *rs1* cDNA fragment. The PCR fragment amplified from 3′-RACE (770 bp) contained the chicken *rs1* cDNA fragment, stop codon, 3′-untranslated region, and poly(A) tail. There were two bands from the 5′-RACE assay (about 1.1 kb and 330 bp). Both PCR fragments were subcloned and sequenced. The 1.1-kb fragment was nonspecific PCR amplification of ribosomal RNA. The smaller fragment included the chicken *rs1* cDNA fragment (AI438129), start codon, 5′-untranslated region, and poly(G) primer sequence.

The complete chicken retinoschisin sequence contained 856 nucleotides encoding 225 amino acids (Tables 1 and 2). Amino

TABLE 2

Retinoschisin protein alignment

Shown is a homology comparison of human (*Homo*), mouse (*Mus*), and chicken (*Gallus*) retinoschisin amino acid sequences. Highly conserved identical sequence (*), conserved substitutions (:), and semiconserved substitutions (.) are shown.

```
Homo     MSRKIEGFLLLLLFGYEATLGLSSTEDEGEDPWYQKACKCDCQGGPNALWSAGATSLDCI 60
Mus      MPHKIEGFFLLLLFGYEATLGLSSTEDEGEDPWYQKACKCDCQVGANALWSAGATSLDCI 60
Gallus   MRFKMGRVLLSLLFWYKAVLALSPGEDERLELWHSKACKCNCQGGPNSVWSSGTNSLECM 60
         *  *:  .:* *** *:*.*.**. ***  : *:.*****:** *.*::**:*:.**:*:

Homo     PECPYHKPLGFESGEVTPDQITCSNPEQYVGWYSSWTANKARLNSQGFGCAW-LSKFQDS 119
Mus      PECPYHKPLGFESGEVTPDQITCSNPEQYVGWYSSWTANKARLNSQGFGCAW-LSKYQDS 119
Gallus   PECPYHKPLGFESGAVTPDQISCSNPEQYTGWYSSWTANKARLNGQGFGCALALSKYQDN 120
         ************** ******:*******.**************.******  ***:**.

Homo     SQWLQIDLKEIKVISGILTQGRCDIDEWMTKYSVQYRTDERLNWIYYKDQTGNNRVFYGN 179
Mus      SQWLQIDLKEIKVISGILTQGRCDIDEWVTKYSVQYRTDERLNWIYYKDQTGNNRVFYGN 179
Gallus   GQWLQIDLKEVKVISGILTQGRCDADEWMTKYSVQYRTDENLNWVYYKDQTGNNRVFYGN 180
         .*********:************ ***:***********.***:***************

Homo     SDRTSTVQNLLRPPIISRFIRLIPLGWHVRIAIRMELLECVSKCA 224
Mus      SDRSSTVQNLLRPPIISRFIRLIPLGWHVRIAIRMELLECASKCA 224
Gallus   SDRSSSVQNLLRPPIVARYIRLIPLGWHVRIAIRMELLECLGKCG 225
         ***:*:*********::*:********************* .**.
```

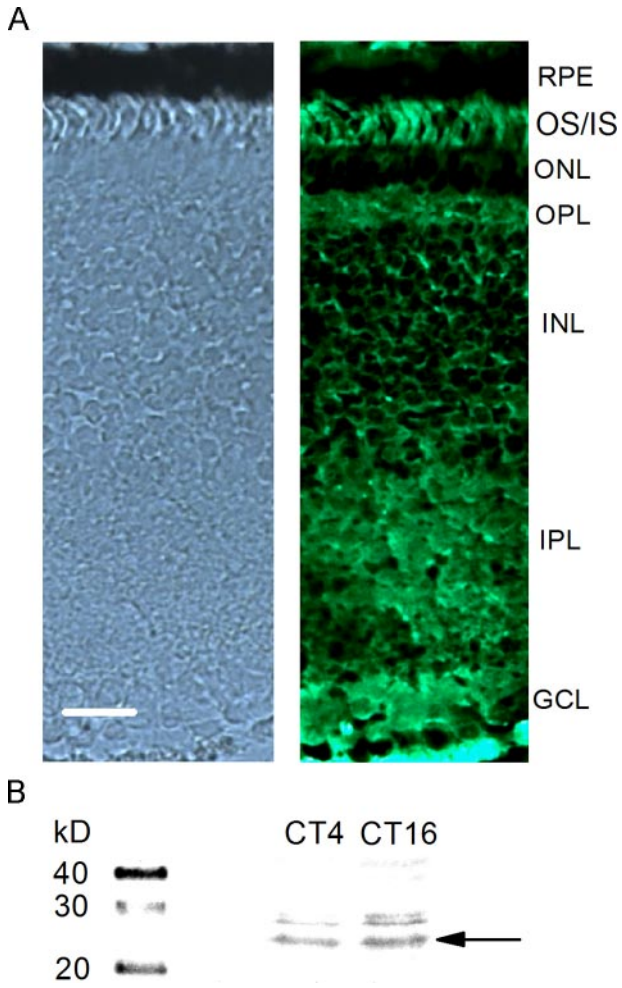

FIGURE 1. **The distribution of retinoschisin protein in the chick retina.** *A*, the *left panel* shows a bright field light microscopy image, and the *right panel* shows a fluorescence image stained with anti-retinoschisin antibody (Santa Cruz Biotechnology). The tissue section was 10 μm thick. *RPE*, retina pigment epithelium; *OS/IS*, outer and inner segments of photoreceptors; *ONL*, outer nuclear layer; *OPL*, outer plexiform layer; *INL*, inner nuclear layer; *IPL*, inner plexiform layer; *GCL*, ganglion cell layer. *Bar*, 20 μm. *B*, the Western blot result shows the circadian regulation of retinoschisin expression in the chick retina. Whole retinas were collected at CT 4 (subjective day) and CT 16 (subjective night). The anti-retinoschisin antibody (Santa Cruz Biotechnology) labeled two bands at 24 and 28 kDa. The protein amount of retinoschisin is higher at CT 16 than CT 4.

acid sequence alignment among human (*Homo*), mouse (*Mus*), and chicken (*Gallus*) showed that the N-terminal (first 60 aa) of chicken *rs1* was only moderately homologous to the mouse and human (~50%). The remainder of chicken *rs1* (including the functional discoidin domain) showed nearly 90% homology to the human and mouse (Table 2). The full-length nucleotide sequence of chicken retinoschisin (*rs1*) has been submitted to the GenBank^{TM} data base under accession number EU924185.

To further verify *rs1* protein expression in the chicken retina, we used a commercially available retinoschisin antibody for immunohistochemical staining and immunoblotting of E18 chick retinas (Fig. 1). The retinoschisin antibody (H-65) recognizes amino acids (aa) 126–190 of the mouse and human that is also conserved in chicken *rs1*. Two bands were observed from chicken whole retina lysate immunoblotting results, a major band around 24 kDa and a minor band around 28 kDa (Fig. 1*B*). The protein expression of retinoschisin was higher during the subjective night (CT 16) than during the subjective day (CT 4; Fig. 1*B*). This observation is consistent with the findings we previously have shown that the protein expression of retinoschisin is under the circadian control with a peak at CT 16 and a nadir at CT 4 using an antibody developed in the Trump laboratory with the retinoschisin band around 24 kDa (26). We also found that the distribution of retinoschisin protein in the chick retina (Fig. 1*A*) was similar to that in mammals (8, 15, 33). The distribution of retinoschisin protein was most prominent on the photoreceptor outer and inner segments (*OS/IS*), whereas outer and inner plexiform layers (*OPL* and *IPL*) also showed heavier staining (Fig. 1*A*). The immunofluorescence signal was weaker in the outer and inner nuclear layers (*ONL* and *INL*). From our cloning and morphological data, we are confident that chicken retinoschisin shares similar functional characteristics with its mouse and human counterparts.

L-type VGCCs Regulate the Circadian Secretion of Retinoschisin—We previously established that VGCCα1D and retinoschisin proteins are expressed in a circadian fashion in retina cells with a peak during the subjective night and a nadir during the subjective day (25, 26). To independently assess the relative amount of retinoschisin bound to the cell surface and that found in the cytoplasm, a cell surface biotinylation assay was performed (Fig. 2). The relative amount of retinoschisin binding to the cell surface of retinal photoreceptors increased as time passed from day to night (Fig. 2, *A* and *B*). Nitrendipine (3 μM) treatment for 2 h significantly decreased retinoschisin binding to the cell surface at CT 17 back to daytime levels but did not affect retinoschisin binding at CT 5 (Fig. 2, *A* and *B*), and at this concentration, nitrendipine specifically blocks L-type VGCCs (25, 34). Interestingly, cytosolic retinoschisin levels appeared to remain constant throughout the day, and nitrendipine did not alter these levels (Fig. 2*C*). Whole lysate (cell surface plus cytosolic) analysis of photoreceptor retinoschisin (Fig. 2*D*) revealed a similar pattern to that seen in Fig. 2*A*. Samples not exposed to biotin treatment showed no binding of retinoschisin to the streptavidin-linked agarose beads (data not shown). The results showed that L-type VGCCs affected membrane-bound retinoschisin. Hence, we set forth to further investigate whether there was any physical interaction between the VGCCα1 subunit and retinoschisin using co-IP and mammalian two-hybrid assays.

VGCCα1D Interacts with Retinoschisin—Since the VGCCα1D antibody (Alomone) only matches 12 of 17 residues in the chicken VGCCα1D, we first verified the specificities and affinities of the VGCCα1 antibodies. The VGCCpanα1 antibody (Alomone) that recognizes all rat VGCCα1 subtypes (α1A, 1B, 1C, 1D, 1E, 1F, and 1S) was selected as a positive control. The epitope of this antibody is completely homologous with the chicken VGCCα1D and -α1C. Fig. 3*A* shows that both anti-VGCCα1D and VGCCpanα1 antibodies were able to detect a strong band slightly above 200 kDa and a nonspecific band close to 140 kDa. Results from both antibodies showed that the protein expression of VGCCα1D (*arrows*) was under circadian control, with higher expression during the subjective night (CT 17) than during the subjective day (CT 5), as we previously reported (25). It is worth noting that VGCCα1D antibodies

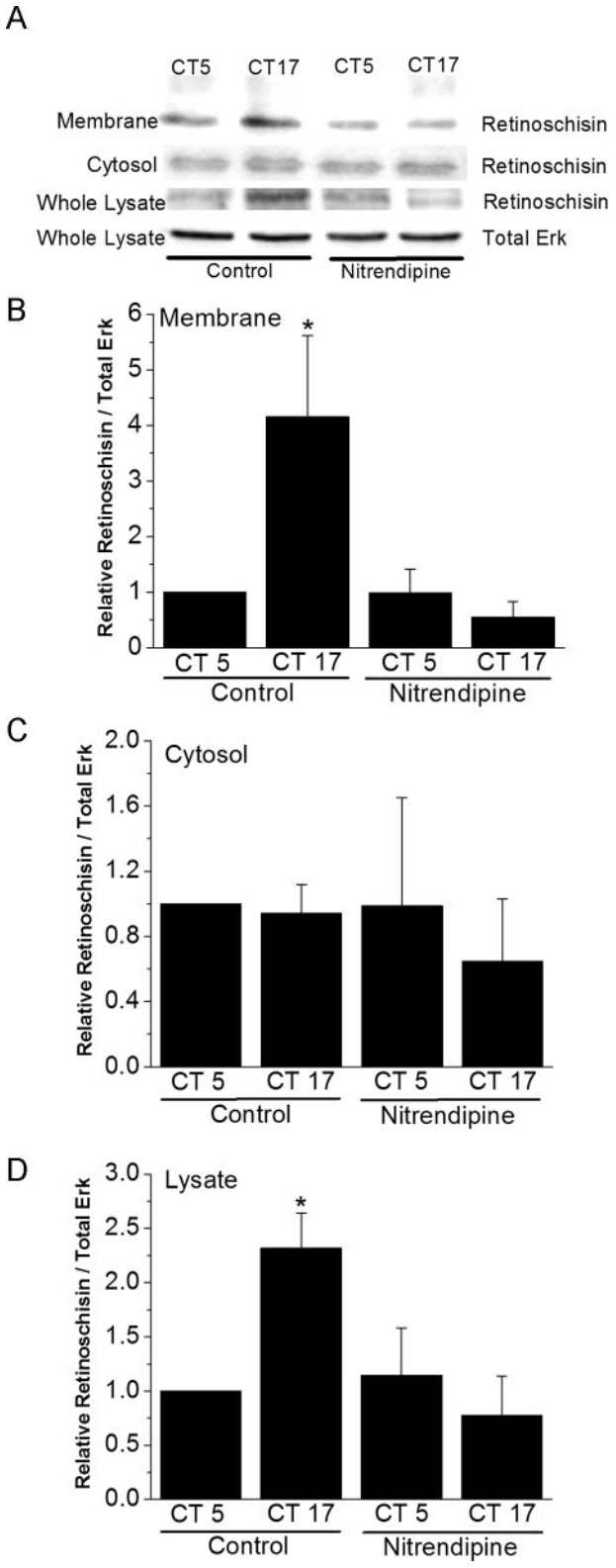

FIGURE 2. **Circadian regulation of retinoschisin in the retina is gated by L-type VGCCs.** After biotin labeling of cell surface proteins, retinoschisin content at the cell surface (membrane-bound), in the cytoplasm, or in the whole cell lysate was independently analyzed using Western immunoblotting. The retinoschisin antibody was produced in the Trump laboratory. *A*, immunoblots show retinoschisin in the membrane-bound, cytosolic, and whole lysate fractions as well as the total Erk in the whole lysate (loading control). *B*, the amount of retinoschisin bound to the cell surface is significantly higher during the subjective night than during the subjective day. Nitrendipine, an L-type VGCC inhibitor, abolishes the circadian nature of retinoschisin binding to the cell surface. *C*, retinoschisin content of the cytoplasm does not change as a function of circadian time and is not affected by nitrendipine treatment. *D*, retinoschisin content of the whole lysate (cell surface plus cytosolic) resembles the data in *B*. $n = 5–6$ for each group. *, $p < 0.05$ was regarded as significant.

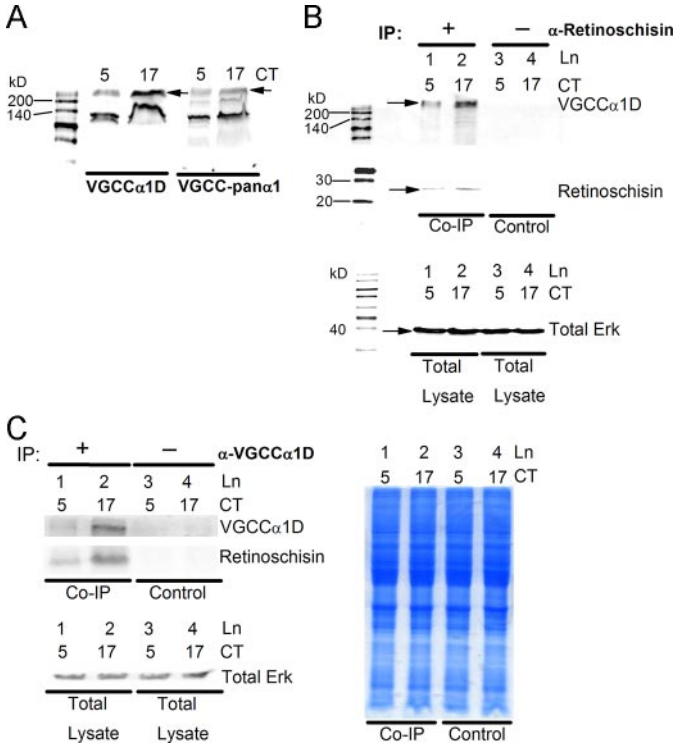

FIGURE 3. **Determination of whether a physical interaction between retinoschisin and VGCCα1D exists by co-immunoprecipitation.** *A*, an anti-VGCCpanα1 antibody was used to verify the effectiveness of labeling chicken VGCCα1D by an anti-VGCCα1D antibody. Both antibodies are able to detect a strong band slightly above the 200 kDa marker. The *arrows* indicate the protein expression of VGCCα1D. Both antibodies show that the protein expression of VGCCα1D is higher during the subjective night (CT 17) than during the subjective day (CT 5). *B*, co-IP experiment using an anti-retinoschisin antibody (produced in the Trump laboratory) to co-precipitate VGCCα1D. Samples were collected at CT 5 and CT 17. *Lanes 1* and *2*, retinoschisin expression is higher during the subjective night, and more VGCCα1D co-precipitates with retinoschisin at CT 17. *Lanes 3* and *4*, control groups with no anti-retinoschisin antibody show almost no binding of retinoschisin or VGCCα1D to Protein A-agarose beads. *C*, co-IP experiment using a VGCCα1D antibody (Alomone) to co-precipitate retinoschisin. *Lanes 1* and *2*, VGCCα1D expression is higher during the subjective night, and more retinoschisin co-precipitates with VGCCα1D at CT 17. *Lanes 3* and *4*, control groups with no VGCCα1D antibody show almost no binding of VGCCα1D or retinoschisin to Protein A-agarose beads. Western blot analysis of total Erk in the sample lysates used in the co-IP experiments in *B* and *C* show that total protein between samples is fairly even (in *lower panels* of *B* and *C*). A Coomassie Blue-stained gel of sample lysates used in the co-IP experiments also shows an even amount of total protein between samples (*right* panel). $n = 3$ for each group.

from other companies did not produce results as esthetically pleasing as Alomone's antibodies for our experiments. Therefore, we chose Alomone's anti-VGCCα1D for our co-immunoprecipitation studies. The anti-retinoschisin antibody generated in the Trump laboratory was used to immobilize retinoschisin to Protein A-agarose beads to co-precipitate VGCCα1D subunits (Fig. 3*B*). We previously showed that retinoschisin and VGCCα1D are expressed more abundantly during the subjective night. Here, our co-IP results showed increased binding of retinoschisin to the agarose beads during this time (Fig. 3*B*, *middle*). In our control

groups where normal rabbit serum was introduced to the sample preparation, virtually no retinoschisin binding to the beads occurred. At both CT 5 and CT 17, VGCCα1D subunits co-precipitated with retinoschisin, with a higher amount during the subjective night (CT 17). As with retinoschisin, VGCCα1D showed no nonspecific binding to the agarose beads (Fig. 3*B*, *top*). In the reverse scenario, co-immunoprecipitation experiments using the anti-VGCCα1D antibody to pull down retinoschisin showed similar results (Fig. 3*C*). A Coomassie-stained gel of the lysates used in Fig. 3*C* (*left*) and a Western blot of total Erk, which does not change throughout the day (25, 27, 28, 30), demonstrated even total protein amounts used in the various co-IP groups.

Retinoschisin Interacts with the N-terminal Region of VGCCα1D—To verify the interaction between retinoschisin and L-type VGCCα1D subunits, the mammalian two-hybrid assay was selected for this study. The full-length chicken *rs1* cDNA was inserted into the pBIND vector, which encoded a recombinant protein with GAL4 DNA binding domain as the bait. The L-VGCCα1D fragments were amplified and inserted into the pACT vector, which encoded a protein containing a VP16 activation domain (Fig. 4*A*). The intracellular C-terminal fragment of VGCCα1D contained 500 aa located toward the -COOH end, whereas the N-terminal fragment of VGCCα1D contained 500 aa, including the short N terminus, the first repeat motif (I, containing six transmembrane segments), and a partial junction sequence between the first (I) and second (II) repeats (Fig. 4*A*). The pG5Luc contained five tandem GAL4 binding sequences upstream of a luciferase coding region and was used to report protein interactions. The relative luciferase activities were at least three times higher in co-transfection with pBIND-*rs1*, pACT-L-VGCCα1D N terminus, and pG5Luc in comparison with the controls (Fig. 4*B*). Neither pACT-L-VGCCα1D C terminus nor pBIND alone showed significant luciferase activities compared with other groups. These results demonstrate that chicken retinoschisin specifically binds the N-terminal region of L-type VGCCα1D.

Retinoschisin Modulates the Circadian Rhythm of L-type VGCC Currents—Given that L-type VGCCα1D subunits directly interact with retinoschisin, we next investigated the biological function of this interaction and whether retinoschisin might contribute to the circadian rhythm of L-type VGCCs. We transfected cultured photoreceptors with plasmids encoding GFP and a missense retinoschisin mutant or with GFP alone using a biolistic transfection method. Transfections were performed after the cells were entrained to LD 12:12 for 5 days, thus ensuring that disruption of retinoschisin genes would not affect circadian entrainment of the cells. On the second day of DD, whole-cell recordings were obtained from cones during the subjective day (CT 4–7) or subjective night (CT 16–19). There was no difference in the circadian rhythmicity between non-transfected cones and cones transfected with GFP alone (data not shown). Hence, we only show controls with photoreceptors transfected with GFP alone. Control cells displayed a normal circadian rhythm of L-type VGCC currents with higher maximum average current amplitude recorded during the subjective night (CT 16–19; 17.2 ± 3 pA, $n = 9$) than recorded during the subjective day (CT 4–7; 8.8 ± 1 pA, $n = 9$; Fig. 5, *A* and *D*). There was no difference in average membrane capacitance

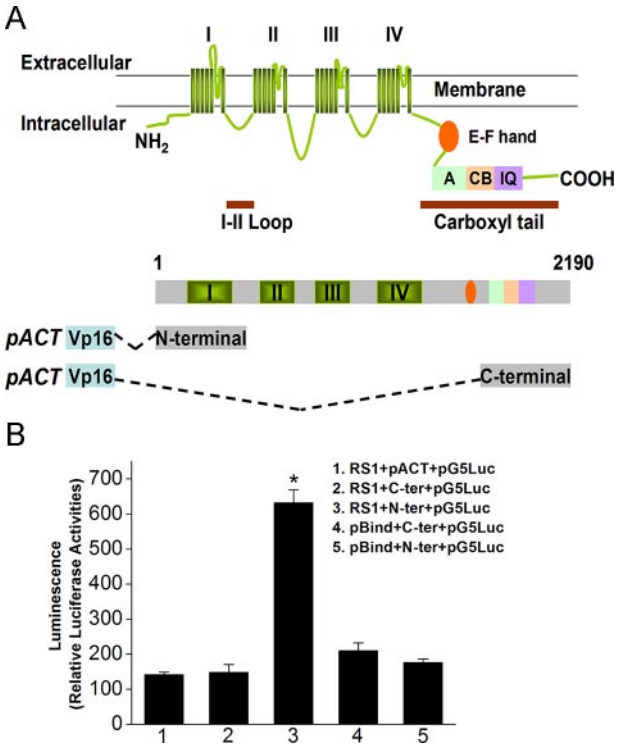

FIGURE 4. **Protein-protein interaction between retinoschisin and VGCCα1D is verified by mammalian two-hybrid assays.** *A*, a schematic model illustrates the structural organization of the L-VGCCα1 subunit and the N- and C-terminal fragments of L-VGCCα1D used for the mammalian two-hybrid assays. The L-VGCCα1 model is modified from Bodi *et al.* (44) and Abernethy and Soldatov (45). The L-VGCCα1 contains four transmembrane repeat motifs (*I*, *II*, *III*, and *IV*). The EF-hand, A, CB, and IQ motifs have specific amino acid sequences that can be phosphorylated by kinases or can bind to calmodulin/calmodulin-like proteins. The N-terminal fragment of L-VGCCα1D containing the first repeat motif (*I*) and the C-terminal fragment of VGCCα1D containing A, C, and IQ motifs were used in the mammalian two-hybrid assays. *B*, group 1 was cells co-transfected with pBind-Rs1 (*RS1*), empty pACT (*pACT*), and pG5Luc reporter (*pG5Luc*). Group 2 was cells co-transfected with pBind-Rs1 (*RS1*), pACT-C terminus of L-VGCCα1D (*C-ter*), and pG5Luc reporter (*pG5Luc*). Group 3 was cells co-transfected with pBind-Rs1 (*RS1*), pACT-N terminus of L-VGCCα1D (*N-ter*), and pG5Luc reporter (pG5Luc). Group 4 was cells co-transfected with empty pBind (*pBind*), pACT-C-terminal of L-VGCCα1D (*C-ter*), and pG5Luc reporter (*pG5Luc*). Group 5 was cells co-transfected with empty pBind (*pBind*), pACT-N terminus of L-VGCCα1D (*N-ter*), and pG5Luc reporter (*pG5Luc*). Results indicated that retinoschisin interacts with the N-terminal of L-VGCCα1D. For each group, $n = 7$, and the relative luciferase activity of each group was expressed as mean ± S.E. *, a statistically significant difference of Group 3 compared with all other groups. Comparisons were made using analysis of variance with Tukey's *post hoc* test; *, $p < 0.005$.

from cells recorded during the subjective day (3.0 ± 0.13 picofarads) or subjective night (3.2 ± 0.09 picofarads). By contrast, photoreceptors co-transfected with GFP and R141G, a missense mutation of retinoschisin, showed no circadian rhythm due to a decrease of L-type VGCC current amplitudes especially during the subjective night (Fig. 5, *B* and *D*). The R141G mutation apparently only affected L-VGCC current amplitudes during the subjective night without changing channel gating kinetics and activation voltage. The R141G mutation does not interfere with retinoschisin secretion but affects the surface residue within the loop region (13, 31) that occurs in human XLRS cases. Interestingly, co-transfection with another XLRS missense mutant gene, W92C, into entrained photoreceptors had no effect on the circadian regulation of L-VGCC currents (Fig. 5, *C* and *D*). This mutation, W92C, causes cysteine-trig-

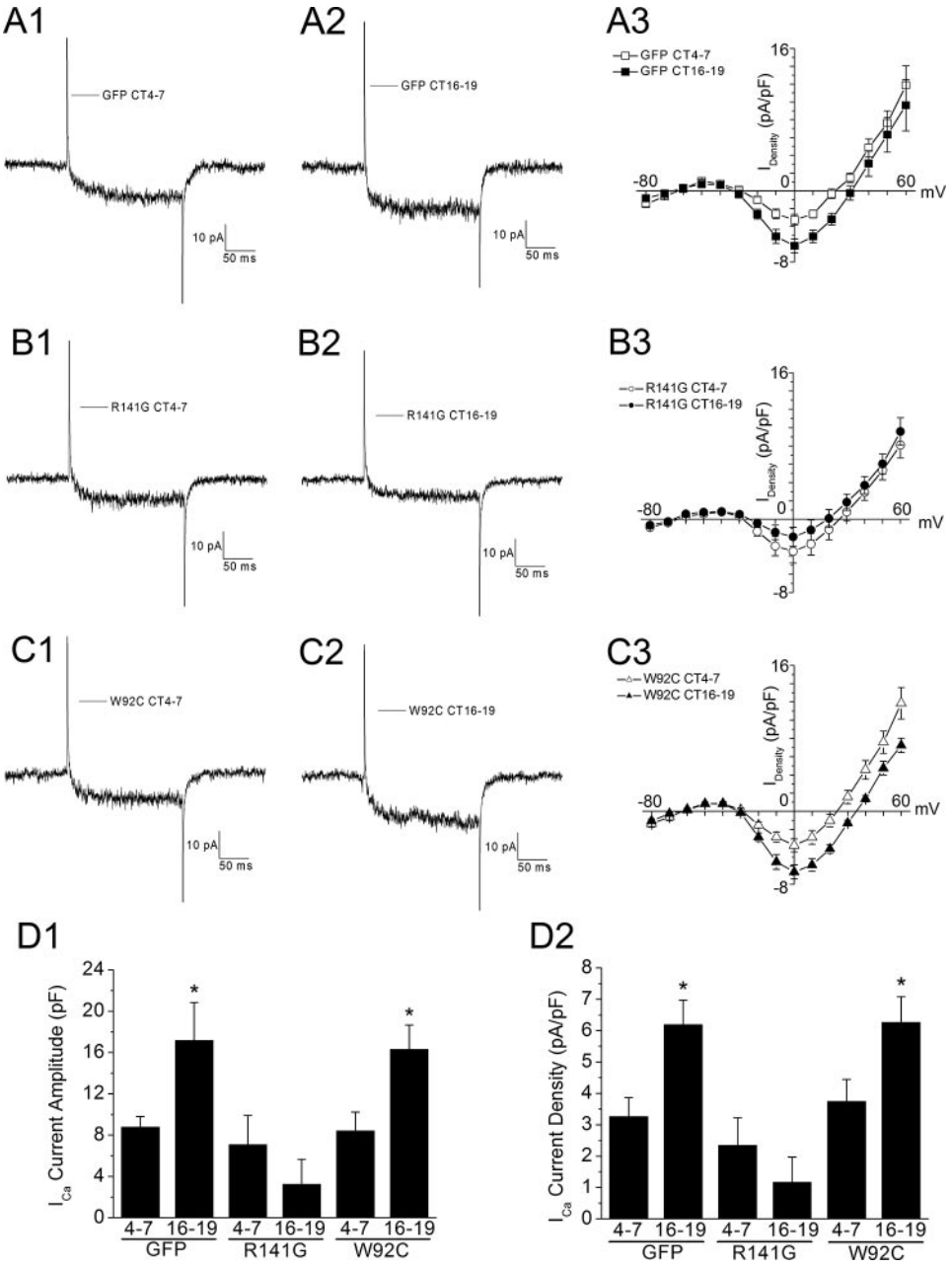

FIGURE 5. **Circadian rhythm of L-type VGCC currents is affected by a specific missense mutation of retinoschisin.** The L-type VGCC currents were recorded from cultured chick cone photoreceptors during the subjective day (CT 4–7) and subjective night (CT 16–19) on the second day of DD after biolistic transfection. All cells were recorded using a 200 ms step command with holding potential at −65 mV and steps from −80 to 60 mV at 10-mV increments. Representative current traces under a step command from −80 to 0 mV are shown (*A1*, *A2*, *B1*, *B2*, *C1*, and *C2*). Averaged current-voltage (*I-V*) relationships were obtained from the step command as in current density (*A3*, *B3*, and *C3*). *A1–A3*, the L-type VGCC currents are under circadian control in cone photoreceptors transfected with empty GFP vector, phrGFPII (*GFP*). *A1* and *A2* are representative current traces recorded during the subjective day (*A1*) and subjective night (*A2*). The maximum current densities (*A3*) are significantly larger when cells were recorded during the subjective night (CT 16–19; *filled squares*) than during the subjective day (CT 4–7; *open squares*) without changes in channel gating properties. *B1–B3*, the circadian rhythm of L-type VGCC currents is dampened in cone photoreceptors co-transfected with R141G (a missense mutation of retinoschisin) and GFP. *B1* and *B2* are representative current traces recorded during the subjective day (*B1*) and subjective night (*B2*). The maximum current densities (*B3*) are smaller when cells were recorded during the subjective night (CT 16–19; *filled circles*) than during the subjective day (CT 4–7; *open circles*). However, the channel gating properties are not altered after co-transfection. *C1–C3*, co-transfection with W92C, another missense mutation of retinoschisin, and GFP into photoreceptors has no effect on the circadian regulation of L-type VGCC currents. *C1* and *C2* are representative current traces recorded during the subjective day (*C1*) and subjective night (*C2*). The maximum current densities (*C3*) are significantly larger when cells were recorded during the subjective night (CT 16–19; *filled triangles*) than during the subjective day (CT 4–7; *open triangles*). *D1* and *D2*, the maximum inward current amplitudes (*D1*) and the maximum inward current densities (*D2*) were elucidated at 0 mV of the step command from −80 mV. Comparisons were made using Student's *t* test between CT 4–7 and CT 16–19 of each transfection condition, $n = 9–18$; *, $p < 0.05$.

gered intermolecular bonding and forms retinoschisin polymers (35) that result in intracellular retention of the mutant retinoschisin (31). Therefore, W92C does not participate in extracellular interactions with L-type VGCCs. In all groups, the voltage that elicited maximum currents did not change, and transfections (with or without mutants) did not alter channel gating kinetics. Both mutant constructs, R141G and W92C, lie within regions of high homology among chickens, mice, and humans.

DISCUSSION

Retinoschisin is believed to play an important role in cell-cell adhesion in development and maintenance of retinal cytoarchitecture (7, 8, 15). However, the concentration of retinoschisin remains high in the photoreceptor layer in adults (33), and recent evidence shows that the pineal glands in rodents and humans also express retinoschisin (36). Furthermore, *rs1* mutations cause structural delamination of the neural retinal layers in mice, but the pineal gland structures remain intact (36). Therefore, retinoschisin may serve roles other than maintaining retina structure. In this study, we provide evidence for a novel role of retinoschisin in the circadian regulation of L-type VGCCs in chick retina photoreceptors. Previously, we showed that the mRNA and protein expression of both retinoschisin and L-VGCCα1D in chick retinas are under circadian control, and the secretion of retinoschisin is higher at night than during the day (25, 26). Although inhibition of L-VGCCs dampens the circadian rhythm of retinoschisin secretion (26) as well as membrane-bound retinoschisin (Fig. 2), inhibition of L-VGCCs does not completely abolish the presence of retinoschisin on the plasma membrane, cytosol, or total lysate (Fig. 2). The L-VGCCs are basically governing the circadian nature of retinoschisin, including its retinal content and secretion (26).

Here, we demonstrate that retinoschisin is a positive feedback to

modulate the circadian rhythm of L-type VGCCs. A specific missense mutation (R141G) that affects the surface residue within the loop region of retinoschisin causing human XLRS significantly decreased L-type VGCC current amplitudes during the subjective night without affecting channel gating kinetics, whereas transfection with another missense mutant gene, W92C, into entrained photoreceptors had no effect on L-VGCC activities (Fig. 5). Since the W92C mutant form of retinoschisin is not secreted (31), it does not have a direct extracellular interaction with VGCCα1 subunits. At the same time, W92C does not interfere with the wild type retinoschisin normally expressed by photoreceptors, and as a result, it does not affect the normal circadian rhythm of L-type VGCCs. On the other hand, the R141G mutant form of retinoschisin would compete with the wild type retinoschisin to bind to L-VGCCα1 subunits; therefore, cells transfected with R141G had significantly decreased L-VGCC current amplitudes during the subjective night. Results from both co-immunoprecipitation (Fig. 3) and mammalian two-hybrid assays (Fig. 4) demonstrated that retinoschisin interacts with VGCCα1D subunits. Hence, retinoschisin may play an important role in stabilizing VGCCα1 subunits that have already been inserted into the plasma membrane. In other words, retinoschisin is crucial in membrane retention of VGCCα1 subunits. The R141G mutation might affect the protein-protein interaction between retinoschisin and VGCCα1 subunits that ultimately leads to decreased membrane retention of L-VGCCs and smaller current amplitudes.

These results advance our understanding of retinoschisin in three ways. First, we provide molecular evidence showing a function of retinoschisin other than maintaining retina cytoarchitecture. Second, our results might explain why the ERGs from XLRS and XLCSNB patients are very comparable with each other (18). Previously, Morgans *et al.* (37) showed that cone photoreceptors have both L-VGCCα1D and -α1F, whereas rods only contain α1F. Although the chicken VGCCα1F sequence is not available, the 500-aa N-terminal fragments of chicken VGCCα1D (gCACNA1d) and human VGCCα1D and -α1F (hCNCNA1d and hCNCNA1f, respectively) are highly conserved (Table 3). For this reason, retinoschisin may interact with both L-type VGCCα1D and -1F subunits in the retina and play an important role in stabilizing all VGCCα1 subunits that have already been inserted into the photoreceptor plasma membrane. Whereas XLCSNB patients have mutations in the L-type VGCCα1F subunit gene (16, 17), XLRS patients might have a deficiency in L-type VGCCα1 insertion into or retention in the plasma membrane due to an *RS1* mutation, thereby providing a possible explanation as to why XLCSNB and XLRS patients have similar abnormal ERGs (18). Third, we provide the first evidence of a bidirectional modulation between an ion channel (L-type VGCCs) and an extracellular protein (retinoschisin); the circadian rhythm of retinoschisin secretion is regulated by L-type VGCCs, whereas secreted retinoschisin has a positive feedback modulation on the circadian rhythm of L-type VGCCs through protein-protein interactions. More specifically, retinoschisin interacts with the N-terminal region of VGCCα1D (Fig. 4*B*). Since our fragment of VGCCα1D N-terminal contained the first repeat motif (I) and a partial junction sequence between the first (I) and second (II) repeats, the interaction between retinoschisin and VGCCα1D is probably derived from the discoidin domain of retinoschisin and the extracellular loop of the first motif of VGCCα1D.

TABLE 3

Homology comparison of the 500-aa N-terminal fragments of human L-type VGCCα1C, -1D, and -1F and chicken α1D sequences

Amino acid alignment of chicken VGCCα1D (gCACNA1d) and human VGCCα1D, -α1C, and -α1F (hCACNA1d, hCACNA1c, and hCACNA1f, respectively) are shown. The highlighted sequence is the 500-aa N-terminal fragment used in the mammalian two-hybrid assays. Highly conserved identical sequence (*), conserved substitutions (:), and semiconserved substitutions (.) are shown.

```
gCACNA1d        --------MQHHQQQQPEQHPEEANYASS--TRIPLPGDGPTTQSNSSAPSKQTVLSWQA 50
hCACNA1d        MMMMMMMKKMQHQRQQQADHANEANYARG--TRLPLSGEGPTSQPNS---SKQTVLSWQA 55
hCACNA1c        ------MVNENTRMYIPEENHQGSNYGSPRPAHANMNANAAAGLAPEHIPTPGAALSWQA 54
hCACNA1f        -----------------MSESEGGKDTTP--EPSPANGAGPGP---------------EW 26
                                 .. : .:           . ..                 :

gCACNA1d        AIDAARQAKAAQNMNTTTAQPVGSLSQRKRQQYAKSKKQGNTSNSRPPRALFCLSLNNPI 110
hCACNA1d        AIDAARQAKAAQTMSTSAPPPVGSLSQRKRQQYAKSKKQGNSSNSRPARALFCLSLNNPI 115
hCACNA1c        AIDAARQAKLMGSAGNATISTVSS-TQRKRQQYGKPKKQGSTTATRPPRALLCLTLKNPI 113
hCACNA1f        GLCPGPPAVEGESSGASGLG-----TPKRRNQHSKHKTVAVASAQRSPRALFCLTLANPL 81
                .: ..  *    . . :        : ::*:*:.* *. . ::  *..***:**:* **:

gCACNA1d        RRACISLVEWKPFDIFILLSIFANCVALAVYIPFPEDDSNSTNHNLEKVEYAFLIIFTVE 170
hCACNA1d        RRACISIVEWKPFDIFILLAIFANCVALAIYIPFPEDDSNSTNHNLEKVEYAFLIIFTVE 175
hCACNA1c        RRACISIVEWKPFEIIILLTIFANCVALAIYIPFPEDDSNATNSNLERVEYLFLIIFTVE 173
hCACNA1f        RRSCISIVEWKPFDILILLLTIFANCVALGVYIPFPEDDSNTANHNLEQVEYVFLVIFTVE 141
                **:***:******:*:***:********.:**********::* ***:*** **:*****

gCACNA1d        TFLKIIAYGLLLHPNAYVRNGWNLLDFVIVVVGLFSVILEQLTKETEGGSHSGGKPGGFD 230
hCACNA1d        TFLKIIAYGLLLHPNAYVRNGWNLLDFVIVIVGLFSVILEQLTKETEGGNHSSGKSGGFD 235
hCACNA1c        AFLKVIAYGLLFHPNAYLRNGWNLLDFIIVVVGLFSAILEQATKAD-GANALGGKGAGFD 232
hCACNA1f        TVLKIVAYGLVLHPSAYIRNGWNLLDFIIVVVGLFSVLLEQGPGRPGDAPHTGGKPGGFD 201
                :.**::****::**.**:*********:**:*****.:*** .    ..   .** .***

gCACNA1d        VKALRAFRVLRPLRLVSGVPSLQVVLNSIIKAMVPLLHIALLVLFVIIIYAIIGLELFIG 290
hCACNA1d        VKALRAFRVLRPLRLVSGVPSLQVVLNSIIKAMVPLLHIALLVLFVIIIYAIIGLELFIG 295
hCACNA1c        VKALRAFRVLRPLRLVSGVPSLQVVLNSIIKAMVPLLHIALLVLFVIIIYAIIGLELFMG 292
hCACNA1f        VKALRAFRVLRPLRLVSGVPSLHIVLNSIMKALVPLLHIALLVLFVIIIYAIIGLELFLG 261
                ***********************:.:*****:**:**************************:*

gCACNA1d        KMHKSCFLID--SDILVEEDPAPCAFS-GNGRQCVMNGTECKGGWVGPNGGITNFDNFAF 347
hCACNA1d        KMHKTCFFAD--SDIVAEEDPAPCAFS-GNGRQCTANGTECRSGWVGPNGGITNFDNFAF 352
hCACNA1c        KMHKTCYNQEGIADVPAEDDPSPCALETGHGRQCQN-GTVCKPGWDGPKHGITNFDNFAF 351
hCACNA1f        RMHKTCYFLG--SDMEAEEDPSPCASS-GSGRACTLNQTECRGRWPGPNGGITNFDNFFF 318
                :***:*:     :*: .*:**:*** . * ** *    * *:  * **: ******** *

gCACNA1d        AMLTVFQCITMEGWTDVLYWVNDAIGCEWPWIYFVSLIILGSFFVLNLVLGVLSGEFSKE 407
hCACNA1d        AMLTVFQCITMEGWTDVLYWVNDAIGWEWPWVYFVSLIILGSFFVLNLVLGVLSGEFSKE 412
hCACNA1c        AMLTVFQCITMEGWTDVLYWVNDAVGRDWPWIYFVTLIIIGSFFVLNLVLGVLSGEFSKE 411
hCACNA1f        AMLTVFQCVTMEGWTDVLYWMQDAMGYELPWVYFVSLVIFGSFFVLNLVLGVLSGEFSKE 378
                ********:***********:**:* : **:***:*:*:********************

gCACNA1d        REKAKARGDFQKLREKQQLEEDLKGYLDWITQAEDIDPENDEEAD-----EEGKRNRVT 461
hCACNA1d        REKAKARGDFQKLREKQQLEEDLKGYLDWITQAEDIDPENEEEGG-----EEGKRN--- 463
hCACNA1c        REKAKARGDFQKLREKQQLEEDLKGYLDWITQAEDIDPENEDEGM-----DEEKPR--- 462
hCACNA1f        REKAKARGDFQKQREKQQMEEDLRGYLDWITQAEELDMEDPSADDNLGSMAEEGRAGHRP 438
                ************ *****:****:**********::* *: .          :* :

gCACNA1d        LADLMEEKKKSRLSCFGRSS------NKHASMPTSETESVNTENV 500
hCACNA1d        ----------------------------TSMPTSETESVNTENV 479
hCACNA1c        ---------------------------NMSMPTSETESVNTENV 479
hCACNA1f        QLAELTNRRRGRLRWFSHSTRSTHSTSSHASLPASDTGSMTETQG 483
                                          *:*:*:* *:.  :
```

In addition, known modulation mechanisms of L-type VGCCα1 subunits are at the C-terminal regulatory domain involving phosphorylation, dephosphorylation, binding with calmodulin or calmodulin-like proteins, or variable length of the C-terminal due to alternative splicing (38–43). However, all of these modulations change channel gating kinetics including shifts in activation voltages with or without affecting the maximum current amplitudes (38–43). Our results demonstrate that interaction between retinoschisin and the N-terminal region of VGCCα1D does not change the channel gating kinetics but only affects channel insertion/retention into the plasma membrane, since transfection with the R141G mutant only decreased current amplitudes without shifting the activation voltage and the voltage that elicited maximum currents. This observation further illustrates the importance of extracellular matrix proteins in stabilizing/anchoring plasma membrane insertion/retention of ion channels. Further investigation using a point mutation strategy will give us a more accurate picture of specific interacting sites between retinoschisin and VGCCα1D.

Our full-length sequence of chicken retinoschisin (Tables 1 and 2) showed that retinoschisin is highly conserved. Humans, mice, and chickens share 90% homology in the retinoschisin C-terminal region, which forms the functional discoidin domain (9, 11). In addition, the distribution of retinoschisin protein in chick retina (Fig. 1) is very similar to the pattern described in mammals (8, 15, 33). These results indicate that retinoschisin is very important in retina function and physiology across species. In summary, we demonstrated that functional expression of two molecules, L-type VGCCs and retinoschisin, is under circadian control (25, 26). The protein-protein interactions between VGCCα1D and retinoschisin have a positive feedback regulation on each other. This circadian-governed reciprocal regulation between L-type VGCCs and retinoschisin in photoreceptors provides a local mechanism that may stabilize circadian oscillations in the retina and, therefore, allow visual systems to anticipate daily changes in ambient illumination over 10–12 orders of magnitude (19, 20, 25).

Acknowledgments—We thank Drs. Tao Wang and Lindsay Gleghorn in the Trump laboratory for preparation of retinoschisin antibody and mutant constructs (R141G and W92C). We thank Dr. Robert Burghardt (Director of the Image Analysis Laboratory, College of Veterinary Medicine and Biomedical Sciences at Texas A&M University) for assistance in using the imaging facility. We also thank Drs. Paul Hardin, William Griffith, Brian Perkins, and Evelyn Tiffany-Castiglioni for critical comments on the manuscript.

REFERENCES

1. Wu, X., Davis, G. E., Meininger, G. A., Wilson, E., and Davis, M. J. (2001) *J. Biol. Chem.* **276,** 30285–30292
2. Waitkus-Edwards, K. R., Martinez-Lemus, L. A., Wu, X., Trzeciakowski, J. P., Davis, M. J., Davis, G. E., and Meininger, G. A. (2002) *Circ. Res.* **90,** 473–480
3. Gui, P., Wu, X., Ling, S., Stotz, S. C., Winkfein, R. J., Wilson, E., Davis, G. E., Braun, A. P., Zamponi, G. W., and Davis, M. J. (2006) *J. Biol. Chem.* **281,** 14015–14025
4. Evers, M. R., Salmen, B., Bukalo, O., Rollenhagen, A., Bosl, M. R., Morellini, F., Bartsch, U., Dityatev, A., and Schachner, M. (2002) *J. Neurosci.* **22,** 7177–7194
5. Grayson, C., Reid, S. N., Ellis, J. A., Rutherford, A., Sowden, J. C., Yates, J. R., Farber, D. B., and Trump, D. (2000) *Hum. Mol. Genet.* **9,** 1873–1879
6. Molday, L. L., Hicks, D., Sauer, C. G., Weber, B. H., and Molday, R. S. (2001) *Invest. Ophthalmol. Vis. Sci.* **42,** 816–825
7. Reid, S. N., Akhmedov, N. B., Piriev, N. I., Kozak, C. A., Danciger, M., and Farber, D. B. (1999) *Gene* (*Amst.*) **227,** 257–266
8. Reid, S. N., Yamashita, C., and Farber, D. B. (2003) *J. Neurosci.* **23,** 6030–6040
9. Molday, R. S. (2007) *Exp. Eye Res.* **84,** 227–228
10. Gehrig, A., Weber, B. H., Lorenz, B., and Andrassi, M. (1999) *J. Med. Genet.* **36,** 932–934
11. Molday, L. L., Wu, W. W., and Molday, R. S. (2007) *J. Biol. Chem.* **282,** 32792–32801
12. Tantri, A., Vrabec, T. R., Cu-Unjieng, A., Frost, A., Annesley, W. H., Jr., and Donoso, L. A. (2004) *Surv. Ophthalmol.* **49,** 214–230
13. Wang, T., Waters, C. T., Rothman, A. M., Jakins, T. J., Romisch, K., and Trump, D. (2002) *Hum. Mol. Genet.* **11,** 3097–3105
14. Zeng, Y., Takada, Y., Kjellstrom, S., Hiriyanna, K., Tanikawa, A., Wawrousek, E., Smaoui, N., Caruso, R., Bush, R. A., and Sieving, P. A. (2004) *Invest. Ophthalmol. Vis. Sci.* **45,** 3279–3285
15. Reid, S. N., and Farber, D. B. (2005) *Glia* **49,** 397–406
16. Bech-Hansen, N. T., Naylor, M. J., Maybaum, T. A., Pearce, W. G., Koop, B., Fishman, G. A., Mets, M., Musarella, M. A., and Boycott, K. M. (1998) *Nat. Genet.* **19,** 264–267
17. Strom, T. M., Nyakatura, G., Apfelstedt-Sylla, E., Hellebrand, H., Lorenz, B., Weber, B. H., Wutz, K., Gutwillinger, N., Ruther, K., Drescher, B., Sauer, C., Zrenner, E., Meitinger, T., Rosenthal, A., and Meindl, A. (1998) *Nat. Genet.* **19,** 260–263
18. Bradshaw, K., Allen, L., Trump, D., Hardcastle, A., George, N., and Moore, A. (2004) *Doc. Ophthalmol.* **108,** 135–145
19. Cahill, G. M., and Besharse, J. C. (1995) *Prog. Retinal Eye Res.* **14,** 267–291
20. Green, C. B., and Besharse, J. C. (2004) *J. Biol. Rhythms* **19,** 91–102
21. Barnes, S., and Kelly, M. E. (2002) *Adv. Exp. Med. Biol.* **514,** 465–476
22. Ivanova, T. N., and Iuvone, P. M. (2003) *Brain Res.* **973,** 56–63
23. Ivanova, T. N., and Iuvone, P. M. (2003) *Brain Res.* **991,** 96–103
24. Hull, C., Studholme, K., Yazulla, S., and von Gersdorff, H. (2006) *J. Neurophysiol.* **96,** 2025–2033
25. Ko, M. L., Liu, Y., Dryer, S. E., and Ko, G. Y. (2007) *J. Neurochem.* **103,** 784–792
26. Ko, M. L., Liu, Y., Shi, L., Trump, D., and Ko, G. Y. (2008) *Invest. Ophthalmol. Vis. Sci.* **49,** 1615–1621
27. Ko, G. Y., Ko, M. L., and Dryer, S. E. (2001) *Neuron* **29,** 255–266
28. Ko, G. Y., Ko, M. L., and Dryer, S. E. (2004) *J. Neurosci.* **24,** 1296–1304
29. Chae, K. S., and Dryer, S. E. (2005) *J. Neurochem.* **94,** 367–379
30. Ko, G. Y., Ko, M. L., and Dryer, S. E. (2003) *J. Neurosci.* **23,** 3145–3153
31. Wang, T., Zhou, A., Waters, C. T., O'Connor, E., Read, R. J., and Trump, D. (2006) *Br. J. Ophthalmol.* **90,** 81–86
32. Gleason, E., Mobbs, P., Nuccitelli, R., and Wilson, M. (1992) *Vis. Neurosci.* **8,** 315–327
33. Takada, Y., Fariss, R. N., Tanikawa, A., Zeng, Y., Carper, D., Bush, R., and Sieving, P. A. (2004) *Invest. Ophthalmol. Vis. Sci.* **45,** 3302–3312
34. Ko, G. Y., Ko, M., and Dryer, S. E. (2004) *Brain Res.* **1021,** 277–280
35. Wu, W. W., Wong, J. P., Kast, J., and Molday, R. S. (2005) *J. Biol. Chem.* **280,** 10721–10730
36. Takada, Y., Fariss, R. N., Muller, M., Bush, R. A., Rushing, E. J., and Sieving, P. A. (2006) *Mol. Vis.* **12,** 1108–1116
37. Morgans, C., Bayler, P., Oesch, N., Ren, G., Akileswaran, L., and Taylor, W. (2005) *Vis. Neurosci.* **22,** 561–568
38. Dzhura, I., Wu, Y., Colbran, R. J., Balser, J. R., and Anderson, M. E. (2000) *Nat. Cell Biol.* **2,** 173–177
39. Dzhura, I., Wu, Y., Colbran, R. J., Corbin, J. D., Balser, J. R., and Anderson, M. E. (2002) *J. Physiol.* (*Lond.*) **545,** 399–406
40. Dzhura, I., Wu, Y., Zhang, R., Colbran, R. J., Hamilton, S. L., and Anderson, M. E. (2003) *J. Physiol.* (*Lond.*) **550,** 731–738
41. Haeseleer, F., Imanishi, Y., Maeda, T., Possin, D. E., Maeda, A., Lee, A., Rieke, F., and Palczewski, K. (2004) *Nat. Neurosci.* **7,** 1079–1087
42. Norris, C. M., Blalock, E. M., Chen, K. C., Porter, N. M., and Landfield, P. W. (2002) *Neuroscience* **110,** 213–225
43. Singh, A., Gebhart, M., Fritsch, R., Sinnegger-Brauns, M. J., Poggiani, C., Hoda, J. C., Engel, J., Romanin, C., Striessnig, J., and Koschak, A. (2008) *J. Biol. Chem.* **283,** 20733–20744
44. Bodi, I., Mikala, G., Koch, S. E., Akhter, S. A., and Schwartz, A. (2005) *J. Clin. Invest.* **115,** 3306–3317
45. Abernethy, D. R., and Soldatov, N. M. (2002) *J. Pharmacol. Exp. Ther.* **300,** 724–728